Soil wind erosion in ecological olive trees in the Tabernas desert (S.E. Spain): a wind tunnel experiment.

Carlos Asensio[1*], Francisco Javier Lozano[1], Pedro Gallardo[1], Antonio Giménez[2]

[1] Departamento de Agronomía, CEIA3, Campus de Excelencia Internacional en Agroalimentación, Universidad de Almería, Spain.
[2] Departamento de Ingeniería, Universidad de Almería, Spain.

Correspondence to: Carlos Asensio (casensio@ual.es)

Abstract. Wind erosion is a key component of the soil degradation processes. The purposes of this study were to find out the influence of material loss from wind on soil properties for different soil types and changes in soil properties in olive groves when they are tilled. The study area is on the property of an olive oil company and is located in the north of the Tabernas Desert, in Almeria Province, Spain. The climate is semiarid thermomediterranean and it is one of the driest areas in Europe. We used a new wind tunnel model over three different soil types (Calcisol, Cambisol and Luvisol) and concentrated on micro-plot losses and deposits detected by a laser scanner integrated in the tunnel. We also studied the image processing possibilities for examining the particles attached to collector plates located at the end of the tunnel to determine their characteristics, and whether they were applicable to the setup. Samples collected in the traps at the end of the tunnel were analyzed. We paid special attention to the influence of organic carbon, carbonate and clay contents because of their special impact on soil crusting and the wind-erodible fraction. A Principal Components Analysis (PCA) was done to estimate any relationships on generated dust properties and the intensity and behavior of those relationships. Component C1 separated data with high N and OC contents from samples high in Fine silt, $CO_3^=$ and Available K_2O content. C2 separated data with high Coarse silt and Clay contents from data with high Fine sand. C3 was an indicator of Available P_2O_5 content. Then analysis of variance (ANOVAs) were done to analyze the effect of soil type and sampling height on different properties of capted dust. Calculations based on tunnel data showed overestimation of erosion in tilled Cambisol compared to the other tilled soil typologies and calculation of the fraction of soil erodible by wind done by other authors for Spanish soils. As the highest loss was found in Cambisols, mainly due to the effect on soil crusting and the wind-erodible fraction aggregation

of $CaCO_3$, a Stevia cover crop was planted between the rows in this soil type and this favored retention of particles in vegetation.

Keywords: Soil fertility; Laser scanner; Semiarid environment; Tilled soils.

1 Introduction

Soil is the key component of the Earth System as it controls the hydrological, erosional, biological and geochemical cycles, and also contributes with services, goods and resources to the humankind (Keesstra et al., 2012; Brevik et al., 2015; Smith et al., 2015). Soil degradation is related to soil compaction, loss of vegetation and organic matter and increase of soil erosion, either by water or wind (Novara et al., 2011; Prosdocimi et al., 2016; Arjmand Sajjadi & Mahmoodabadi, 2016). To research those processes of land degradation will contribute to restore and rehabilitate them and to understand the soil genesis and related process on soil degradation and formation. Wind erosion is a world wide environmental concern (Houyou et al., 2014; Martínez-Graña et al., 2015) but some regions of the world are more affected due to their climatic conditions (Cerdâ et al., 2010; Borrelli et al., 2016). In semiarid regions, where the distribution and intensity of precipitation are irregular, wind moves enormous amounts of soil, with the consequential ecological imbalance. Several authors (Liu et al., 2003; López et al., 2000; Li et al., 2004; Gao et al., 2015) have studied the relationships of wind erosion, wind speed, soil typology and vegetation, which affect the quality of soil by modifying the organic carbon content.

Leys et al. (2002) evaluated the wind erosion range based on the effect of dry aggregation levels and percentage of clay. Zobeck et al. (2013) observed that dry mechanical and aggregate stability diminished and erodible material increased as soil organic matter content decreased. Beniston et al. (2015) discuss P losses driven by the transport of the mineral fraction, under different tillage management. Kaiser et al. (2014) mention the stocks of the stable C and N pools were not affected by the tillage intensity but were positively correlated with the stocks of the clay-size fraction, indicating a strong influence of site-specific mineral characteristics on the size of these pools.

Benlhabib et al. (2014) analyzed dryland Mediterranean cultivation systems, discussing and recommending sustainable cultivation technologies which showed a significantly positive effect on crop productivity, yield stability and environmental sustainability. Hevia et al. (2007) found that no-till showed more large aggregates and fewer fine aggregates than traditional tillage. This was also indicated by Gao et al. (2015) and Wang et al. (2015) over soil-conserving tillage in Northern China. Gomesa et al. (2003) observed that soil erodibility by wind under traditional tillage was lower than in conservation tillage, since only a limited amount of material was available to wind erosion due mainly to crusting of the soil surface. Colazo & Buschiazzo (2010, 2015) confirmed that cultivation increased the erodible fraction of soil (EF) and reduced dry aggregate stability (DAS) in medium-textured soils by causing weakening of the soil structure due to loss of organic carbon (OC) and breakup of aggregates. In fine-textured soils, the formation of large resistant aggregates by tilling causes EF and DAS to be more alike than under no-till conditions. According to Rawlins et al. (2015), soils with more stable aggregates have larger disaggregation reduction values. These authors mention soil quality, measured by critical soil physical properties, may decline if the organic carbon concentration is less than a critical threshold. Hagen et al. (2010) observed that tilling ridges are effective for trapping aggregates transported by saltation, but do not usually reduce erosion rates in soil where aggregates transported in suspension predominate.

Feras et al. (2008) demonstrated in a wind tunnel study that sediment traps efficiency depended mainly on particle size and wind speed. Traps placed at different heights can measure vertical sediment flow (Basaran et al., 2011).

Expansion and intensification of olive tree cultivation in Andalusia, especially in the late 18th century, accelerated erosion as a result. The introduction of the use of cover crops in the region due to application of the standards derived from the EU Common Agricultural Policy, involves the need for additional management investment (Gómez et al., 2014). In fact, cultivation of Stevia down the center between rows of olive trees is under study in our experimental area.

Vegetation can diminish soil loss from wind, because it reduces the wind speed and soil erodibility, and traps more eroded material (Touré et al., 2011; Leenders et al., 2011; Lozano el al., 2013; Asensio et al., 2015). Udo & Takewaka (2007), in their wind tunnel experiments, arrived at the conclusion that in addition to density, the height and flexibility of vegetation are essential in determining the effectiveness

in lowering mass transport by wind. Youssef et al. (2012) suggest that the pattern of vegetation in rows parallel to the predominant wind direction lowers total mass transport.

Our objectives here were to: (1) study the influence of material loss on soil properties, (2) compare the differences in soil loss due to the soil type, and (3) observe the changes in generated dust properties when olive groves are tilled.

2 Material and Methods

2.1 Study area

The study area is located in the north of the Tabernas Desert, about 10 km NE of the town of the same name (37º03´N, 22º23´W, 400 m a.s.l.) in Almeria Province, Spain, which is in the Sorbas-Tabernas Basin, south of the Filabres Mountains and partly surrounded by the Betic Mountain Chain. The climate is semiarid thermomediterranean, with a mean annual temperature of 17.8ºC. It is one of the driest areas in Europe, with a mean annual precipitation of 283 mm according to the Tabernas meteorological station records for the last 15 years. Lithological material is predominantly sedimentary, identified as a series of marls in contact with Miocene evaporites. Natural plant communities are comprised of isolated native shrubs surrounded by areas of bare soil colonized by biological crusts and annual plant species (Cantón et al., 2011). The study area is on the property of the "*Oro del Desierto*" olive oil company, which has around 25,000 olive trees of different ages scattered on about 100 hectares surrounded by scrubland and other ecological crops, such as Stevia, almonds and grapes. We concentrated on four-year-old *picual* olive trees drip irrigated. Soils are mainly Calcisols (CL), Cambisols (CM) and Luvisols (LV). Texture is silty clay loam to loamy with 37 to 48% gravel fragments and a weak, coarse subangular blocky to strong, medium angular blocky structure.

2.2 Data acquisition and experimental design

Soil parameters of the different soil types are analyzed, before making applications of artificial wind in the tunnel, in order to get starting data. To analyze the soil volume lost from wind erosion and its effect on the surface microtopography, we tested both crusted and recently tilled soil. The crusted soils were strongly protected from wind erosion, while right after tilling, soils were highly susceptible to it. After tilling, soils tended to recover the physical surface crust within 10 to 12 days, reacquiring extra protection from the wind.

The simulations were done in May 2013 in three plots for each soil type with olive trees, with 7 x 5 m tree spacing, which were only tilled once a year and where the aisles between the rows were very close to the predominant wind direction (there was about a 5º offset in Calcisols). The slopes and lengths of fields of the three experimental plots were 2% and 143 m on CL, 0% and 95 m on CM, and 0% and 152 m on LV.

Our reference for weather records was the Tabernas Meteorological Station (located about 2 km away from the study area), one of the network of automatic stations belonging to the Institute of Agrarian, Fishing Research and Education of Andalusia, IFAPA (http://www.juntadeandalucia.es/agriculturaypesca/ifapa/ria/ servlet/FrontController), which is a dependency of the Andalusian Regional Government.

2.3 Wind tunnel

To monitor wind intensity, as well as direction and shear, we worked with a wind tunnel with laminar and turbulent flow similar to real wind conditions, in which the material transported was collected in traps for study. Our tunnel has two parts, as shown in Figure 1, each of which has different functions based on their components. Part 1 shows a generator which provides the energy necessary for the industrial fan which is the first component. The fan blows air into a folding tube structure, providing an air flow which combines laminar and turbulent flows as it passes through an intermediate honeycomb structure. This part is 2 meters length.

Then comes the tunnel itself (Part 2) which consists of three compartments (0.8x0.8x0.8 m each one) into a telescopic structure:

-The first compartment has a metal sheet completely covering the ground to keep the wind from affecting this area.

-The second compartment is the study area itself (0.8x0.8 m), where wind erosion is actually quantified. This area is equipped with a *PCE-424* hot wire anemometer with 0.1 m·s^{-1} resolution, with which wind speed is monitored. There is also a NextEngine Desktop 3D laser scanner, which is used to find the volume of eroded soil and alterations in the microrelief of the soil. The scanner has an indispensable lifting system which acts as a support structure and enables it to be set at the desired height.

-A liquid latex (Latepren® Rx-505) coating was applied to the soil surface in the third compartment to fix particles so they would not move around during blowing and mix in with the particles in the study zone. This way the natural roughness of the ground was maintained. The latex coating is spread with a bulb shape from outside the third tunnel compartment to avoid return of external particles due to edge turbulence.

At the end of the tunnel, the particles become attached to some vertical adhesive plates placed at different heights (0, 15, 40 and 70 cm), and are later analyzed using an industrial machine vision camera.

There are also particle traps (Fryrear BSNE, adapted for a fixed wind direction) located at the same height as the adhesive plates (Asensio *et al.*, 2015), retain the dust that is later analyzed to quantify the loss. 0 cm one was partially buried, to locate the window at surface level.

The duration of the wind tunnel experiment was ten minutes by using a wind speed of 7.6 m s^{-1} at 70 cm height, following criteria of Fister & Ries (2009). The wind speed value corresponds to the maximum daily average wind speed (last 15 years) registered at 2 m height by Tabernas Station. Flow simulation software, according to 15 cm tunnel rounding radius, shows wind profile homogeneity from 70 cm height to the central part of ground study area, at cross section.

In each case, the ground was scanned twice, before and after simulation with the wind tunnel. Scans were done at a height of 44 cm using a NextEngine 3D laser scanner under conditions of natural dryness. This scanner has shown its applicability in acquiring microreliefs of agricultural soils (Aguilar *et al.*, 2009) in high-precision field work (High Definition mode and MACRO) considering a sample size large enough to represent the plot in great detail. This provides a 120 cm^2 scan area with a 400 ppi capture

density and nominal precision of 0.127 mm. Based on two point clouds found for each plot (before and after wind simulation), two digital terrain models with a 0.1 x 0.1 cm resolution were generated. The eroded soil volume was estimated as the difference in volume between DTMs. Once the soil volume was known, we estimated the amount of soil lost using the bulk density of each soil.

After making applications of artificial wind in the tunnel, we analyze the soil volume lost from wind erosion and its effect on the surface microtopography, both crusted and recently tilled soil. The results of the scans done in the wind tunnel only take the loss model (no deposit model) into account. Deposits would have to be considered along with the loss model for the erosion balance to be more moderate.

To find out how wind erosion modifies surface microtopography, the point cloud from each scan was used to calculate random roughness (RR) in each sample, before and after simulation. RR is defined as the standard deviation from the points within the plot after eliminating the slope effect. But in natural areas with a complex topography or on hillsides with high variability (changes in both flat curvature and profile), the elimination of slope does not eliminate the effects of changes in height caused by roughness factors, such as mounds, curvature or higher-order variations in surface, so the RR index tends to overestimate surface roughness in experimental plots. Therefore, the local RR index (RR_L) estimation method was applied (Rodríguez-Caballero et al., 2012) using Equation (1):

$$RR_L = \sqrt{\sum_{i=1}^{i=Nw} \frac{(Zw - \mu w)^2}{(1 - Nw)}} \qquad [1]$$

Where Nw is the number of points in window w, Zw is the height of each point after eliminating the slope effect and μw is the mean height in window w.

The adhesive plates were analyzed using a machine vision camera (JAI-CM080). This monochrome progressive scan camera with a 1024 x 768 pixel resolution is connected to a computer. During image processing with the "ImageJ" program, the number of particles present in each image can be counted, and the mean size of particles, presence of aggregates or a color histogram of the image can be found.

The possibilities for image processing for detailed examination of particles adhering to the plates were studied. In a first approach, to determine the characteristics and applicability to the setup, a series of images of reference samples was taken to demonstrate system capabilities for:

5 -Colorimetry studies: Quantitative study of the color of adhered particles, changing the color model and using the H component in the HSV model.

-Measurement on image of adhered particles

-Particle count

-Roughness analysis of isolated particles

10 **2.4 Sampling and analytical determinations**

Soil samples were taken from the upper 3 cm. We therefore concentrated on recently tilled soils, from which three repetitions of each soil type were evaluated. When using aggregate stability to assess soil erodibility, samples are usually collected from the plough layer, while soil erosion occurs at the soil 15 surface. Hence, the potential changes in erodibility caused by crusting are ignored (Algayer et al., 2014). Using the sub-crust would have led to greatly over-estimated erodibility.

Ground and collected samples were dried, crushed, and passed through a 2-mm sieve to eliminate large fragments. For both ground and trap samples, particle size distribution was assessed by dry sieving and the Robinson pipette method after eliminating organic matter with H_2O_2 (30%) and dispersion by agitation 20 with sodium hexametaphosphate (10%). The sand fraction was separated by wet sieving, dried in an oven and later fractionated by dry sieving. The organic carbon content (OC) was determined using the Walkley-Black wet digestion method. Total N (N) was calculated from NH_3 volumetry after Kjeldahl digestion. Available soil phosphate (P_2O_5) was calculated by photocolorimetry. Available soil potassium (K_2O) was calculated by flame photometry. To determine bulk density (BD), 100-cm^3 cylinders were used to refer 25 to sample dry weight by cylinder volume.

2.5 Statistical analysis

Data on soil characteristics acquired were examined for any changes or differences. A Principal Components Analysis was done to estimate any relationships on generated dust properties and the intensity and behavior of those relationships. Then an analysis of variance (ANOVA) was done to analyze the effect of soil type on OC and $CO_3^=$ contents and another ANOVA was done to analyze the effect of height on clay content. The variables under study did not require transformation to satisfy the requirements of residual normality or variance homogeneity, so when the ANOVAs showed the effect analyzed to be significant, pairwise comparisons were assessed using the least significant difference test. The level of significance was 0.05 in all tests. All statistical analyses were carried out with *SPSS 20*.

3 Results

At the study area, mean soil characteristics before artificial wind recorded for Calcisols, Cambisols and Luvisols (CL_0, CM_0 and LV_0) are shown in Table 1. Three replicates were taken of each soil type.

Surface stoniness of these soils is high and the average gravel for the different typologies is 37% in CL, 48% in CM and 43% in LV.

In this study, we were concentrating on losses and deposits localized in a micro plot, which is what the laser scanner can detect. The results for the three soil typologies in soil blown with the same wind intensity generated artificially in the tunnel are shown in Table 2.

As an example of the results found by scanning, the digital terrain models and erosion maps for a sample from the Cambisol plot are shown in Figure 2. The variations in random roughness are conditioned by the balance of material lost and deposited.

Some of the results of the image processing plate study are shown below (Figure 3). The results, still being validated, can give us an idea that Calcisols have fewer granulometric fractions susceptible to wind erosion. The three typologies have a clear contrast in color conditioned by their clay content and the presence of iron oxides, which makes them darker. In Calcisols, the aggregating effect of $CaCO_3$ may be seen even with the naked eye.

Figure 3 shows large-sized particles, plant residue and, in the color analysis, two groups of materials with different colorimetry.

The samples collected in the traps at the end of the tunnel were also analyzed. A Principal Components Analysis (PCA) of the results was performed using the R correlation matrix. The variables included in the PCA were Fine sand, Very Fine sand, Coarse silt, Fine silt, Clay, OC, N, Available P_2O_5, Available K_2O and $CO_3^=$. First, eigenvalues were calculated and used to decide how many components should be extracted to adequately explain the data. Only the first three roots were worth exploring further, because the rest of them were less than 1. The first three roots account for 81.091% of the variance.

The factors extracted were rotated by Varimax to simplify the interpretation of the Pearson's correlation coefficients of the principal component scores and the raw data. Figure 4 (a) shows the correlation coefficients on the plane of Components 1 and 2. From this figure, it is obvious that the % Fine silt, % $CO_3^=$ and Available K_2O variables are clearly negatively associated with Component C1 while % N and % OC are associated positively with C1. Thus C1 separates data with high N and OC contents from samples high in Fine silt, $CO_3^=$ and Available K_2O content. Component C2 is negatively associated with Fine sand and positively associated with % Coarse silt and % Clay. C2 separates data with high Coarse silt and Clay contents from data with high Fine sand.

Figure 4 (b) shows the correlation coefficients on the plane of Components 1 and 3, where it may be observed that Component 3 is positively associated with Available P_2O_5. Therefore C3 is an indicator of Available P_2O_5 content.

Figure 5 show how samples cluster around the three main components. Figure 5 (a) shows that C1 is strongly related to the soil group, that is, C1 separates the three groups of soil, and so the contents of the variables associated with C1 differentiate groups of soil. Thus from Figure 5 (a), the dust samples belonging to the CL group are the highest in Available K_2O content, while data for LV show high content in N.

Furthermore, C2 is related to the sampling height and separates 0 and 15 cm from 40 and 70 cm. Therefore, the lower heights are associated with higher content in Fine sand while higher heights are associated with more content in Coarse silt and Clay.

Figure 5 (b) shows that C3 separates soil Groups CL and LV from CM, suggesting that Available P_2O_5 content is the major difference.

Special attention should be paid PCA results for OC, $CO_3^=$ and Clay contents because of their special impact on soil crusting and the wind-erodible fraction. Variables OC and $CO_3^=$ were associated with Component C1, which is strongly related to soil type. So we tested the effects of soil type on OC and $CO_3^=$ contents with an analysis of variance (ANOVA). Furthermore, the Clay variable was associated with Component C2, which was related to the height, and therefore, we tested the effect of height on Clay content. We did not need to apply transformations to satisfy the requirements of residual normality and variance homogeneity.

The ANOVA table for collected dust samples from different Soil Types (Table 3) applied to % OC and % $CO_3^=$ shows significant differences for soil provenance in two variables. When its effect was found to be significant in the ANOVAs, and as none was considered the reference soil, we performed pairwise comparisons of the three soils. These were assessed using the least significant difference test (LSD, $P \leq 0.05$). Table 4 show that samples with the highest OC content were from CM, but with no significant difference from LV. From CL had significantly lower OC than the other two soil types where this variable was similar. $CO_3^=$ contents were significantly different in the three soil types and CL had the highest % $CO_3^=$ while LV had the lowest.

The ANOVA table for height (Table 3) applied to % Clay shows significant differences too, but this time we did not do pairwise comparisons of all the four heights, but analyzed for a significant difference in heights of 0-15 cm and 40-70 cm. From Table 5, the difference between heights of 0 to 15 and 40 to 70 is referred in Eq. (2):

$$L = \frac{1}{2}(23.844 + 23.811) - \frac{1}{2}(26.900 + 28.900) = -4.0725 \tag{2}$$

As t is 7.0912 (t=4.0725/0.5743) with a p-value of P=4.811713e-08, the difference between the heights of 0-15 and 40-70 is highly significant.

We were also interested in the comparison between heights of 0 and 15 cm and between 40 and 70 cm. As seen in Table 5, the difference between 0 and 15 cm is clearly not significant, whereas the difference between 40 and 70 is significant, and the highest content of Clay was at a height of 70 cm.

4 Discussion

Soil erosion is currently a major cause of land degradation and relevant at the European and global level. Therefore more studies are needed to improve current models and integrate plot and regional studies to assist decision making (Panagos et al., 2012; Panagos et al., 2014; Borrelli et al., 2015).

As suggested by Lozano et al. (2013) and Asensio et al. (2015), bulk density is doubly influenced, on one hand it tends to be reduced by the effect of organic enrichment, but on the other, increased by the accumulation of fine materials. This has great influence in physical soil crusting. Organic matter often combines with fine soil particles and Zhao et al. (2009) found a correlation coefficient between clay and organic matter content of 0.95.

The availability of phosphates to plants is influenced by factors such as neighboring plants and seasonal dynamics in this semiarid environment. Zhang et al. (2014) made reference to damages by windblown sand and Zhao et al. (2007) showed that the effect of small deposits of sand on soil properties and performance of vegetation were not significant, although the soil temperature tended to rise with increasing thickness of deposits, which could affect the decomposition of organic matter.

According to PCA, Component 1 separates data with high OC contents from high $CO_3^=$ content and Component 3 is an indicator of Available P_2O_5 content, being able to establish differences on soil Groups. C1 separates the three groups of soil, and samples belonging to the LV group show high content in OC. C2 is related to the sampling height and show how higher heights are associated with more content in Clay. ANOVA shows significant differences for CM and LV in front of CL in OC content. We also find significant differences in Clay content for heights of 40-70 cm.

It is well known that velocity threshold increases as the particle size is increases. We did not take into account aggregate size for dust capted samples because these were crushed and passed through a 2-mm sieve for chemical analysing. The soil fraction erodible by wind (EF) is a key parameter for estimating

soil susceptibility to wind erosion. Fryrear et al. (1994) proposed a multiple regression equation for calculating EF which considers the organic matter, sand, silt, clay and calcium carbonate contents as predictive variables. In fact, it has been included in prediction models such as the current Revised Wind Erosion Equation, RWEQ. Calculation of the EF in Spanish soils is problematic due to their high content in $CaCO_3$ (López et al., 2007), so the equation proposed is: EF = 4.77 + 7.43 sand/clay + 27.6/organic matter. Average EF calculated this way for our soils shows a slightly higher result in Cambisols (31%, compared to 27% in Calcisols and Luvisols).

Making a comparison for crusted and tilled soil types on the average soil loss, the tilling loss increase from CL more than six times in CM and more than fourteen times in LV. But this is taking into account only a loss model, without the deposition one.

Image analysis is a useful tool enabling submillimetric particles to be counted, and to analyze their size, shape and color. This could lead to creation of a database of soils with objectively measurable visual characteristics in the mid-term.

As the highest loss was found in Cambisols, a Stevia cover crop has been planted between the rows in this soil type (Figure 1). Stevia cultivation can offer up to three crops a year, which is done manually for leaf that after drying is crushed.This crop favored retention of particles in vegetation, on the property subject of study.

5 Conclusions

Tilled soils in olive groves show a direct relationship between the differences in OC and clay content after blowing. Cambisols are more eroded than Calcisols and Luvisols, mainly due to the effect on soil crusting and the wind-erodible fraction aggregation of $CaCO_3$ in CL and Clay in LV.

The wind tunnel led to overestimation of differences in soil type loss compared to other EF evaluation methods. We could suggest that higher-precision data have been found with this new wind tunnel than found with other any tunnel designed to date, due to high resolution of the devices used, such as laser scanner and particle imaging.

Where wind erosion is higher, it is recommended that cover crops be planted between the rows of olive trees.

Acknowledgments

The authors are grateful to S. Martínez (Dept. of Mathematics, University of Almería) for advice and comments on a previous version of this manuscript and J.A. Torres (Dept. of Computing, University of Almería) for help with image analysis. Also to Deborah Fuldauer for the English language revision. This study was funded by the Andalusia Regional Government (RNM 3614 grant), and European Union ERDF

10   funds.

References

Aguilar, M. A., Aguilar, F., Negreiros, J. Off-the-shelf scanning and close-range digital photogrammetry for measuring
15   agricultural soils microrelief. Biosystem Engineering, 103(4), 504-517. doi:10.1016/j.biosystemseng.2009.02.010, 2009.

Algayer, B., Wang, B., Bourennane, H., Zheng, F., Duval, O., Li, G., Le Bissonnais, Y., Darboux, F. Aggregate stability of a crusted soil: differences between crust and sub-crust material, and consequences for interrill erodibility assessment. An example from the Loess Plateau of China. European Journal of Soil Science, 65 (3), 325-335. doi:10.1111/ejss.12134, 2014.

20 Arjmand Sajjadi, S., Mahmoodabadi, M. Aggregate breakdown and surface seal development influenced by rain intensity, slope gradient and soil particle size, Solid Earth, 6 (1), pp. 311-321. doi: 10.5194/se-6-311-2015, 2015.

Asensio, C., Lozano, F.J., Ortega, E., Kikvidze, Z. Study on the effectiveness of an agricultural Technique based on aeolian deposition, in a semiarid environment. Environmental Engineering and Management Journal, 14 (5), 1143-1150, 2015.

Basaran, M., Erpul, G., Uzun, O., Gabriels, D. Comparative efficiency testing for a newly designed cyclone type sediment trap
25   for wind erosion measurements. Geomorphology, 130, 343-351. doi:10.1016/j.geomorph.2011.04.016, 2011.

Beniston, J.W., Shipitalo, M.J., Lal, R., Dayton, E.A., Hopkins, D.W., Jones, F., Joynes, A., Dungait, J.A.J. Carbon and macronutrient losses during accelerated erosion under different tillage and residue management. European Journal of Soil Science, 66 (1), 218-225. doi:10.1111/ejss.12205, 2015.

Benlhabib, O., Yazar, A., Qadir, M., Lourenço, E., Jacobsen, S. E. How Can We Improve Mediterranean Cropping Systems?
30   Journal of Agronomy and Crop Science, 200 (5), 325-332, 2014.

Borrelli, P., Panagos, P., Ballabio, C., Lugato, E., Weynantgs, M., Montanarella, L. Towards a Pan-European assessment of land susceptibility to wind erosion. Land Degradation & Development, 27 (4), 1093-1105. doi:10.1002/ldr.2318, 2016.

Borrelli, P., Panagos, P., Montanarella, L. New insights into the geography and modelling of wind erosion in the European agricultural land. Application of a spatially explicit indicator of land susceptibility to wind erosion. Sustainability 7, 8823-8836. doi:10.3390/su7078823, 2015.

Brevik, E. C., Cerdà, A., Mataix-Solera, J., Pereg, L., Quinton, J. N., Six, J., and Van Oost, K. The interdisciplinary nature of soil. Soil, 1, 117-129. doi:10.5194/soil-1-117-2015, 2015.

Canton, Y., Sole-Benet, A., de Vente, J., Boix-Fayos, C., Calvo-Cases, A., Asensio, C., Puigdefábregas, J. A review of runoff generation and soil erosion across scales in semiarid south-eastern Spain. Journal of Arid Environments, 75, 1254-1261. doi:10.1016/j.jaridenv.2011.03.004, 2011.

Cerdà A, Hooke J, Romero-Diaz A, Montanarella L, Lavee H. Preface. Soil erosion on Mediterranean type-ecosystems. Land Degradation & Development 21: 71-74. doi:10.1002/ldr.968, 2010.

Colazo, J.C., Buschiazzo, D.E. Soil dry aggregate stability and wind erodible fraction in a semiarid environment of Argentina. Geoderma, 159, 228-236. doi:10.1016/j.geoderma.2010.07.016, 2010.

Colazo, J.C., Buschiazzo, D.E. The Impact of Agriculture on Soil Texture Due to Wind Erosion. Land Degradation & Development, 26 (1), 62-70. doi:10.1002/ldr.2297, 2015.

Feras, Y., Erpul, G., Bogman, P., Cornelis, W.M., Gabriels, D. Determination of efficiency of Vasaline slide and Wilson and Cook sediment traps by wind tunnel experiments. Environmental Geology, 55, 741-757, 2008.

Fister, W., Ries, J.B. Wind erosion in the central Ebro Basin under changing land use management. Field experiments with a portable wind tunnel. Journal of Arid Environments, 73, 996-1004. doi:10.1016/j.jaridenv.2009.05.006, 2009.

Fryrear, D.W., Krammes, C.A., Williamson, D.L., Zobeck, T.M. Computing the wind erodible fraction of soils. J. Soil Water Conservation, 49, 183-188, 1994.

Gao, Y., Dang, X., Yu, Y., Li, Y., Liu, Y., Wang, J. Effects of Tillage Methods on Soil Carbon and Wind Erosion. Land Degradation & Development. doi:10.1002/ldr.2404, 2015.

Gomesa, L., Arrúe, J.L., López, M.V., Sterk, G., Richard, D., Gracia, R., Sabre, M., Gaudichet, A., Frangi, J.P. Wind erosion in a semiarid agricultural area of Spain: the WELSONS project. Catena, 52, 235-256. doi:10.1016/S0341-8162(03)00016-X, 2003.

Gómez, J. A., Infante-Amate, J., González de Molina, M., Vanwalleghem, T., Taguas, E. V., Lorite, I. Olive Cultivation, its Impact on Soil Erosion and its Progression into Yield Impacts in Southern Spain in the Past as a Key to a Future of Increasing Climate Uncertainty. Agriculture, 4, 170-198, 2014.

Hagen, L.J., van Pelt, S., Sharratt, B. Estimating the saltation and suspension components from field wind erosion. Aeolian Research, 1, 147-153. doi:10.1016/j.aeolia.2009.08.002, 2010.

Hevia, G.G., Mendéz, M.J., Buschiazzo, D.E. Tillage affects soil aggregation parameters linked with wind erosion. Geoderma, 140, 90-96. doi:10.1016/j.geoderma.2007.03.001, 2007.

Houyou, Z., Bielders, C.L., Benhorma, H.A., Dellal, A., Boutemdjet, A. Evidence of strong land degradation by wind erosion as a result of rainfed cropping in the algerian steppe: A case study at laghouat. Land Degradation & Development. doi:10.1002/ldr.2295, 2014.

Kaiser, M., Piegholdt, C., Andruschkewitsch, R., Linsler, D., Koch, H.-J., Ludwig, B. Impact of tillage intensity on carbon and nitrogen pools in surface and sub-surface soils of three long-term field experiments. European Journal of Soil Science, 65 (4), 499-509. doi:10.1111/ejss.12146, 2014.

Keesstra, S.D., Geissen, V., van Schaik, L., Mosse., K., Piiranen, S. Soil as a filter for groundwater quality. Current Opinions in Environmental Sustainability, 4, 507-516. doi:10.1016/j.cosust.2012.10.007, 2012.

Leenders, J.K., Sterk, G., Van Boxel, J.H. Modelling wind-blown sediment transport around single vegetation elements. Earth Surface Processes and Landforms, 36 (9), 1218-1229. doi:10.1002/esp.2147, 2011.

Leys, J. F. Erosion by Wind, Effects on Soil Quality and Productivity. In Encyclopedia of Soil Science (ed. R Lal), pp. 499-502. Marcel Dekker, New York, 2002.

Li, F.R., Zhao, L.Y., Zhang, T.H. Wind erosion and airborne dust deposition in farmland during spring in the Horqin Sandy Land of eastern Inner Mongolia, China. Soil & Tillage Research, 75, 121-130. doi:10.1016/j.still.2003.08.001, 2004.

Liu, L.Y., Shi, P.J., Zou, X.Y., Gao, S.Y., Yan, P., Li, X.Y., Dong, Z.B.,Wang, J.H. Short-term dynamic of wind erosion of three newly cultivated grassland soils in Northern China. Geoderma, 115, 55-64. doi:10.1016/S0016-7061(03)00075-2, 2003.

López, M.V., Gracia, R., Arrue, J.L. Effects of reduced tillage on soil surface properties affecting wind erosion in semiarid fallow lands of Central Aragon. European Journal of Agronomy, 12, 191-199. doi:10.1016/S1161-0301(00)00046-0, 2000.

López, M.V., de Dios Herrero, J.M., Hevia, G.G., Gracia, R., Buschiazzo, D.E. Determination of the wind-erodible fraction of soils using different methodologies. Geoderma, 139, 407-411. doi:10.1016/j.geoderma.2007.03.006, 2007.

Lozano, F.J., Soriano, M., Martínez, S., Asensio, C. The influence of blowing soil trapped by shrubs on fertility in Tabernas district (SE Spain). Land Degradation & Development, 24, 575-581. doi:10.1002/ldr.2186, 2013.

Martínez-Graña, A.M., Goy, J.L., Zazo, C. Cartographic Procedure for the Analysis of Aeolian Erosion Hazard in Natural Parks (Central System, Spain). Land Degradation & Development, 26 (2), pp. 110-117. doi:10.1002/ldr.2189, 2015.

Novara, A., Gristina, L., Saladino, S.S., Santoro, A., Cerdà, A. Soil erosion assessment on tillage and alternative soil managements in a Sicilian vineyard. Soil & Tillage Research, 117, pp. 140-147. doi:10.1016/j.still.2011.09.007, 2011.

Panagos, P., Meusburger, K., Van Liedekerke, M., Alewell, C., Hiederer, R., Montanarella, L. Assessing soil erosion in Europe based on data collected through a European network. Soil Science and Plant Nutrition, 60 (1), 15-29. doi:10.1080/00380768.2013.835701, 2014.

Panagos P., Van Liedekerke M., Jones A., Montanarella L. European Soil Data Centre: Response to European policy support and public data requirements. Land Use Policy 29, 329-338. doi:10.1016/landusepol.2011.07.003, 2012.

Prosdocimi, M., Cerdà, A.,Tarolli, P. Soil water erosion on Mediterranean vineyards: A review. Catena, 141, 1-21, 2016.

Rawlins, B.G., Turner, G., Wragg, J., McLachlan, P., Lark, R.M. An improved method for measurement of soil aggregate stability using laser granulometry applied at regional scale. European Journal of Soil Science, 66 (3), 604-614. doi:10.1111/ejss.12250, 2015.

Rodríguez-Caballero, E., Cantón, Y., Chamizo, S., Afana, A., y Solé-Benet, A. Effects of biological soil crusts on surface roughness and implications for runoff and erosion. Geomorphology, 145, 81-89. doi:10.1016/j.geomorph.2011.12.042, 2012.

Smith, P., Cotrufo, M.F., Rumpel, C., Paustian, K., Kuikman, P.J., Elliott, J.A., McDowell, R., Griffiths, R.I., Asakawa, S., Bustamante, M., House, J.I., Sobocká, J., Harper, R., Pan, G., West, P.C., Gerber, J.S., Clark, J.M., Adhya, T., Scholes, R.J., Scholes, M.C., Biogeochemical cycles and biodiversity as key drivers of ecosystem services provided by soils. Soil 1, 665-685. doi:10.5194/soil-1-665-2015, 2015.

Toure, A.A., Rajot, J.L., Garba, Z., Marticorena, B., Petit, C., Sebag, D. Impact of very low crop residues cover on wind erosion in the Sahel. Catena, 85 (3), 205-214. doi:10.1016/j.catena.2011.01.002, 2011.

Udo, K., Takewaka, S. Experimental study of blown sand in a vegetated area. Journal of Coastal Research, 23 (5), 1175-1182. doi:10.2112/05-0499.1, 2007.

Wang T., Xue X., Zhou L., Guo J. Combating Aeolian Desertification in Northern China. Land Degradation & Development, 26 (2), 118-132. doi:10. 1002/ldr. 2190, 2015.

Youssef, F., Visser, S. M., Karssenberg, D., Erpul, G., Cornelis, W. M., Gabriels, D., Poortinga A. The effect of vegetation patterns on wind-blown mass transport at the regional scale: A wind tunnel experiment. Geomorphology, 159, 178-188. doi:10.1016/j.geomorph.2012.03.023, 2012.

Zhang K., Qu J., Han Q., Xie S., Kai K., Niu Q., An Z. Wind tunnel simulation of windblown sand along China's Qinghai-Tibet railway. Land Degradation & Development, 25 (3), 244-250. doi:10. 1002/ldr. 2137, 2014.

Zhao, H.L., Zhou, R.L., Drake, S. Effects of aeolian deposition on soil properties and crop growth in sandy soils of northern China. Geoderma, 142, 342-348. doi:10.1016/j.geoderma.2007.09.005, 2007.

Zhao, H.L., He, Y.H., Zhou, R.L., Su, Y.Z., Li, Y.Q., Drake, S. Effects of desertification on soil organic C and N content in sandy farmland and grassland of Inner Mongolia. Catena, 77, 187-191. doi:10.1016/j.catena.2008.12.007, 2009.

Zobeck, T. M., Baddock, M., van Pelt, R. S., Tatarko, J., Acosta-Martinez, V. Soil property effects on wind erosion of organic soils. Aeolian Research, 10, 43-51. doi:10.1016/j.aeolia.2012.10.005, 2013.

Table 1. Initial soil characteristics for Calcisols (CL₀), Cambisols (CM₀) and Luvisols (LV₀) tested.

SOIL TYPE	% Very coarse sand	% Coarse sand	% Medium sand	% Fine sand	% Very fine sand	% Coarse silt	% Fine silt	% Clay
CL_0	0.0+0.0	5.2+0.2	5.5+0.3	1.9+0.1	10.7+0.8	34.7+1.2	18.3+0.8	23.7+1.8
CM_0	0.2+0.0	8.1+0.4	7.6+0.2	8.8+0.4	20.2+0.7	28.4+0.9	7.9+0.5	18.8+0.7
LV_0	0.3+0.1	5.3+0.1	6.1+0.4	8.9+0.6	25.9+1.1	26.8+1.6	6.3+0.2	20.4+1.0

SOIL TYPE	% OC	% N	Available P_2O_5 (mg·100 g^{-1})	Available K_2O (mg·100 g^{-1})	% $CO_3^=$	E.C. (dS·m^{-1})
CL_0	1.04+0.07	0.036+0.005	4+1	28+4	36+3	5.55+0.24
CM_0	1.82+0.14	0.273+0.027	2+0	75+3	20+2	1.47+0.08
LV_0	2.84+0.32	0.195+0.015	5+2	16+2	2+0	4.76+0.41

SOIL TYPE	pH H_2O	pH KCl	pF % H 33 kPa	pF % H 1500 kPa	A.W.C. (mm)	Bulk density (g·cm^{-3})
CL_0	7.78+0.07	7.57+0.09	13.068+0.114	6.966+0.084	11.1+0.2	1.40+0.02
CM_0	8.28+0.09	7.60+0.13	15.450+0.318	8.112+0.128	14.9+0.5	1.35+0.02
LV_0	8.17+0.12	7.63+0.11	29.163+0.527	13.416+0.345	33.1+0.9	1.22+0.01

Data are means ± standard deviation before applying wind in three replicates for each soil type.

10 **Table 2.** Average soil loss and random roughness (RR_L) in Calcisols (CL), Cambisols (CM) and Luvisols (LV) samples.

		EROSION (mm)	EROSION (g·m^{-2})	RR_L	
CL	Crusted	0.54	756	before	2.6
				after	2.36
	Tilled	1.06	1484	before	7.81
				after	7.28
CM	Crusted	0.25	338	before	3.54
				after	3.51
	Tilled	1.83	2471	before	7.47
				after	6.51
LV	Crusted	0.09	110	before	2.45
				after	2.43
	Tilled	1.39	1696	before	7.52
				after	6.18

Table 3. Summary table for the ANOVAs of % OC, % $CO_3^=$ and % Clay.

Source	Degrees of freedom	Sum of squares	Mean square	*F* ratio	*P*
% OC					
Soil	2	3.914	1.957	85.036	0.000
Residuals	33	0.760	0.023		
Total	35	4.674			
% $CO_3^=$					
Soil	2	4167.722	2083.861	143.116	0.000
Residuals	33	480.500	14.561		
Total	35	4648.222			
% Clay					
Height	3	167.252	55.751	18.785	0.000
Residuals	32	94.971	2.968		
Total	35	262.223			

Table 4. Fisher's least significant difference (LSD) post hoc analysis for % OC, % $CO_3^=$ and % Clay in Calcisols (CL), Cambisols (CM) and Luvisols (LV) samples.

Source	Mean difference	LSD	P-Value
% OC			
Soils			
CL vs CM	-0.71167	0.1259	0.000
CL vs LV	-0.68667	0.1259	0.000
CM vs LV	0.02500	0.1259	0.689
% $CO_3^=$			
Soils			
CL vs CM	6.083	3.1694	0.000
CL vs LV	25.250	3.1694	0.000
CM vs LV	19.167	3.1694	0.000
% Clay			
Height			
0 vs 15	0.0333	1.6543	0.968
40 vs 70	-2.0000	1.6543	0.019
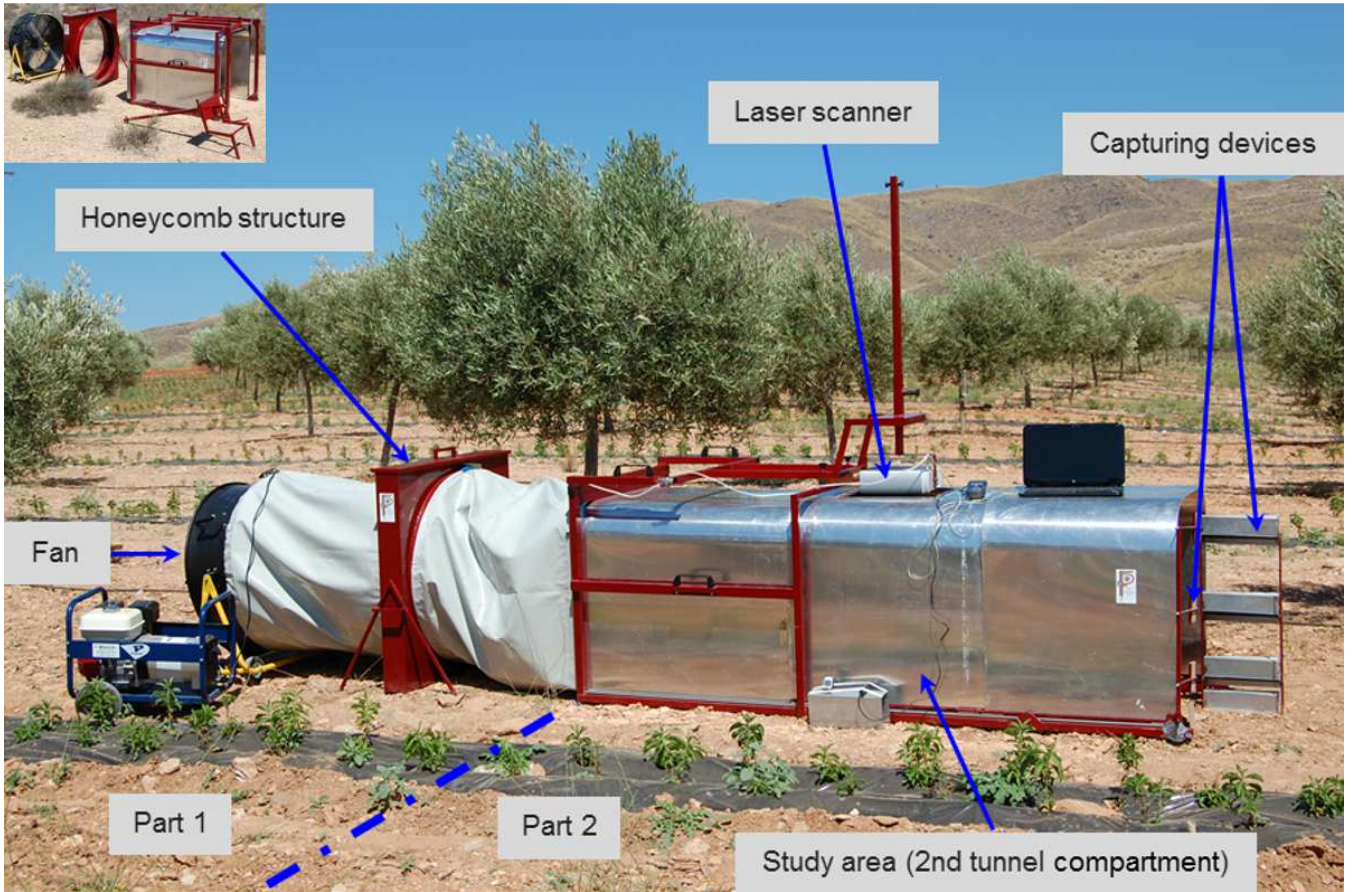
Figure 1. Tunnel arrangement on Cambisol.
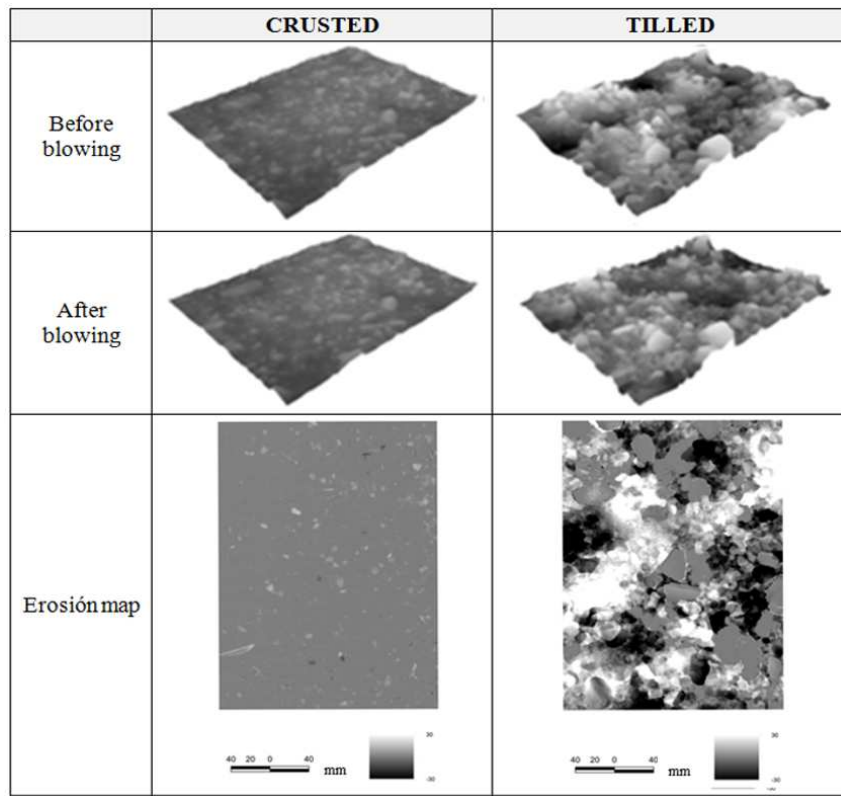
Figure 2. Digital terrain models and erosion maps for a Cambisol.
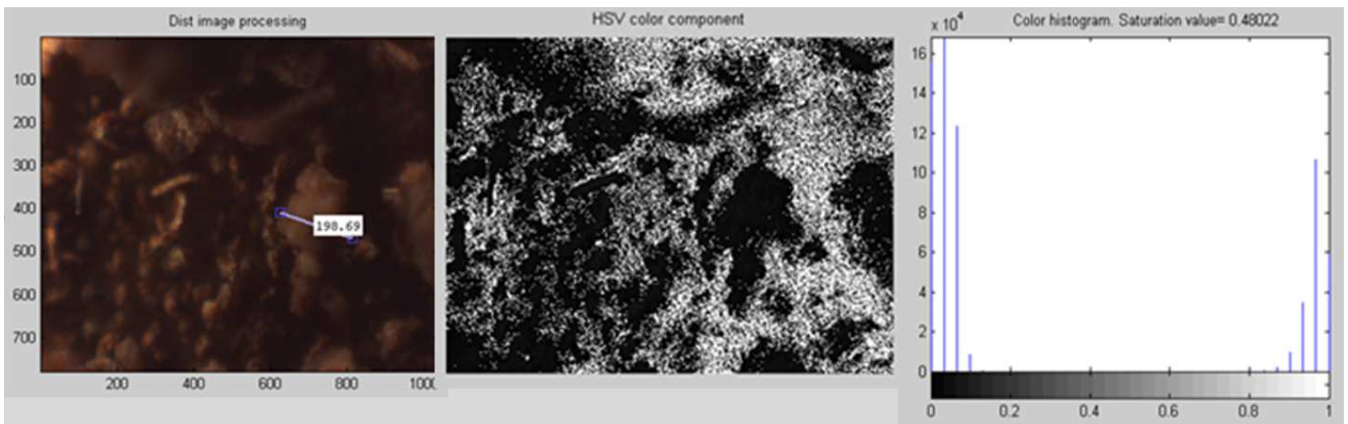
Figure 3. Image of a Luvisol sample, 0 cm height, and pre-processing.
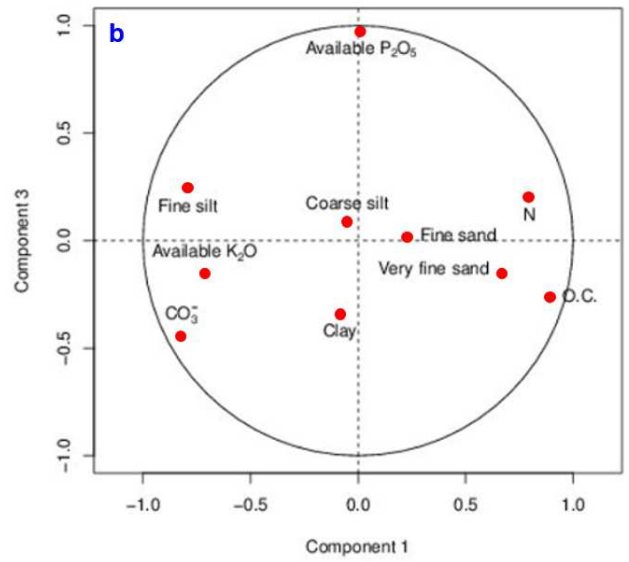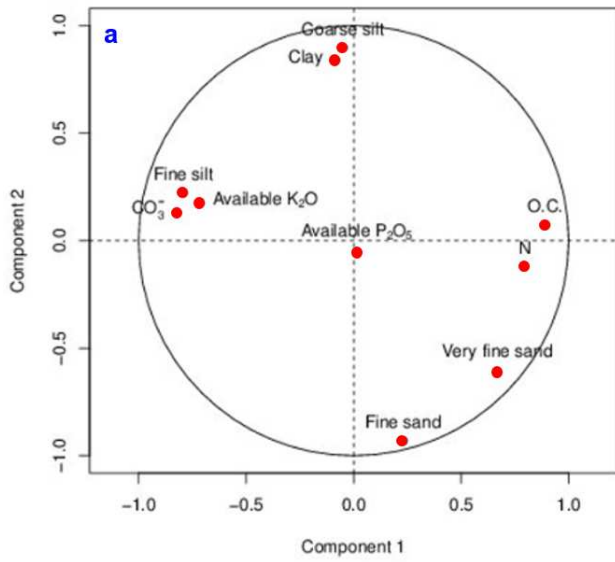
Figure 4. Plot of the correlation coefficients within a unit circle on the plane of Components 1 and 2 (a) and Components 1 and 3 (b).
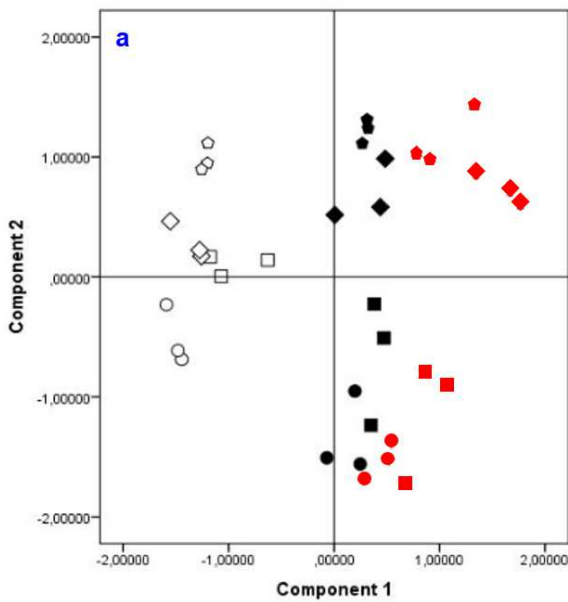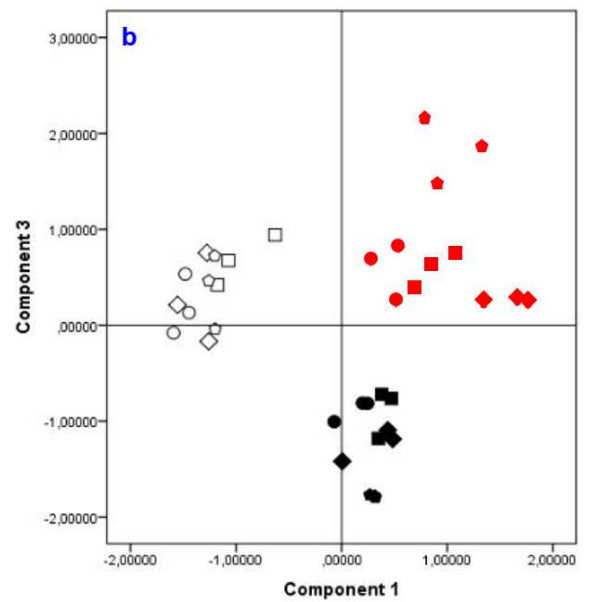
Figure 5. Scatter plot of the height-dust from Calcisols (CL), Cambisols (CM) and Luvisols (LV) categories for the Components 1 and 2 matrix (a) and the Components 1 and 3 matrix (b).